Crack Response to Long-Term Environmental and Blast Vibration Effects

Charles H. Dowding, M.ASCE,[1] and Laureen M. McKenna, P.E., M.ASCE[2]

Abstract: This paper synthesizes seven case histories of micrometer changes in the width of cosmetic cracks in a wide range of wall materials and structure types produced by long term (environmental) and transient (blast vibration) effects. Long term crack response over periods of days to weeks is compared to changes in temperature and humidity. Transient crack response is compared to peak velocity ground motions and structural response. It was found that long term, weather-induced crack response can be more than 1 order of magnitude larger than that induced by noticeable ground motions of 2.5 mm/s (0.1 in./s) and that crack response correlates best with wall shear strains.

DOI: 10.1061/(ASCE)1090-0241(2005)131:9(1151)

CE Database subject headings: Blasting; Vibration; Cracking; Weather; Velocity; Walls; Temperature; Humidity.

Introduction

Advances in sensor technology and computerized data acquisition now permit autonomous measurement of micrometer changes in the width of cosmetic cracks like that shown in Fig. 1. These systems simultaneously monitor crack response to both long-term (environmental) and transient (blast and construction vibration) effects with the same sensor. This information can be downloaded either manually on a periodic basis or combined with telecommunications for near real time display over the Internet to a wide range of interested parties.

This paper synthesizes seven case histories of micrometer crack width response to both long term (environmental) and transient (blast vibration) effects in a wide range of structures. Crack response is compared to ground motions and structural response (the traditional approaches to investigation of cracking potential) as well as changes in temperature and humidity. The paper begins with a description of the structures, vibration environment, genesis of the study, and instruments employed. Response of a distressed wood-framed structure is then employed to describe a typical suite of measurements. Long term crack response over periods of days to weeks is compared to changes in the temperature and humidity. Transient crack response to blast and occupant induced motions is then compared to peak velocity ground motions and structural response where such measurements were made. Finally long term and transient crack responses are compared.

[1]Professor, Dept. of Civil and Environmental Engineering, Northwestern Univ., Evanston, IL 60208-3109 (corresponding author). E-mail: c-dowding@northwestern.edu

[2]Engineer, Shannon and Wilson, Seattle, WA. E-mail: lmm@shanwil.com

Note. Discussion open until February 1, 2006. Separate discussions must be submitted for individual papers. To extend the closing date by one month, a written request must be filed with the ASCE Managing Editor. The manuscript for this paper was submitted for review and possible publication on August 23, 2002; approved on April 5, 2004. This paper is part of the *Journal of Geotechnical and Geoenvironmental Engineering*, Vol. 131, No. 9, September 1, 2005. ©ASCE, ISSN 1090-0241/2005/9-1151–1161/$25.00.

Crack Displacement Sensors

Two types of micrometer crack displacement sensors shown in Fig. 2 have been employed in this study: an eddy current proximity sensor and a linear variable differential transformer (LVDT). Both of these sensors measure changes in crack width. The objective of measurement (with the same sensor) of crack displacements produced by long-term and transient effects is not dependent on the type of sensor. Therefore, any number of sensor types can be employed.

Eddy current proximity devices sense the changes in a magnetic eddy current produced by changes in the distance between the sensor and the target. As shown in the photograph in Fig. 2, two aluminum brackets are epoxied on either side of the crack.

Fig. 1. Photograph of typical crack in wall covering spanned by crack width sensor (inset) along with wires connecting sensors to central data acquisition system at corner of room

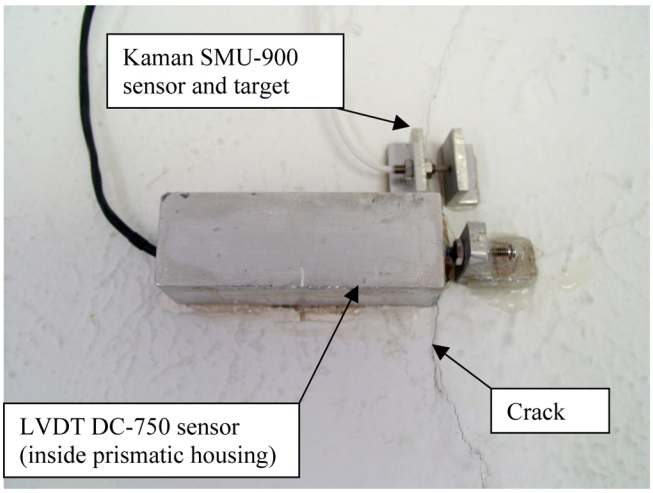

(a)

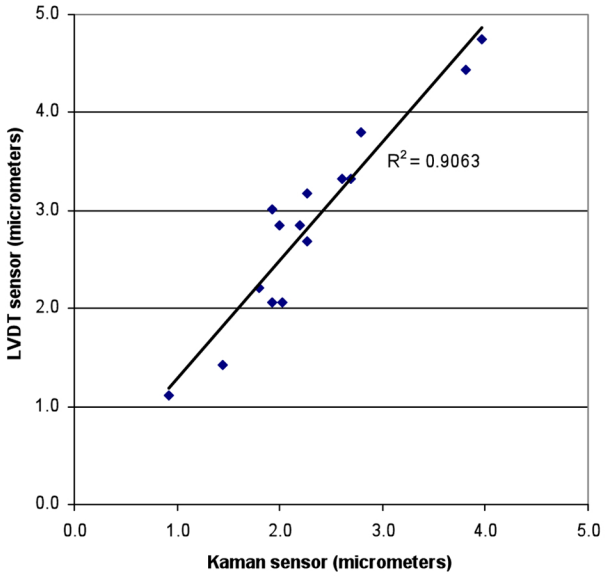

(b)

Fig. 2. Photograph of Kaman and linear variable differential transformer sensors and graphical comparison of peak dynamic response of Kaman and linear variable differential transformer displacement sensors to blast-induced excitation up to 4.5 mm/s (0.18 in./s)

The eddy current device employed in this study, the Kaman 9000 2U, has a displacement range of 508 μm (20 mils) with resolution of 0.1 μm. While the 9000 2U is the more expensive of the Kaman devices, it has the least long-term drift (Siebert 2000).

The LVDT's sense changes the magnetic field in a coil produced by translation of a core magnet attached to the other side of the crack. As shown in the photograph in Fig. 2, the cylindrical LVDT core is epoxied in a prismatic mounting bracket that is in turn epoxied to the wall. Other systems epoxy the LVDT cores directly to the wall. MacroSensors DC 750 and DC-750-125 series LVDTs were employed. They have displacement ranges of ±1,300–3,200 μm with resolutions of 0.4 μm.

Peak response of the LVDT and 9000 2U sensors to both long term and transient, blast-induced response of Crack 1 in structure *C* are remarkably similar. The graph in Fig. 2 compares the peak blast-induced, transient response of the two sensors, and shows that the LVDT and 9000 2U responded consistently at a ratio of 5:4, respectively, for transient events. This difference is the same as observed over time during the long-term comparison of the two sensors (McKenna 2002). Thus the ratio of transient to long-term crack displacement was the same for either sensor. The largest crack (and sensor) response plotted in Fig. 2 is produced by a blast with a peak ground particle velocity of 4.5 mm/s (0.18 in./s).

These systems measure a detailed time history of transient crack response as will be shown later in Fig. 6. The time histories produced by both transducers have similar shapes (McKenna 2002). Given the attachment of the LVDT magnet core to the bracket on the other side of the crack, it was initially believed that crack displacement perpendicular to the wall would have a tendency to press the core against the wall of the coil and reduce its transient response. Apparently the inertia of the wall on opposite sides of the crack is sufficiently large to overcome any such friction, or out of plane motions are small.

A second crack displacement sensor was also affixed to an adjacent, noncracked section of the wall to null out any possible long-term drift and temperature response. The difference in the response of the two sensors (crack sensor minus null sensor) is thus attributed solely to the crack, as described in Siebert (2000), Dowding and Siebert (2001). Null sensor response is typically small. Thus while null sensors are often not needed, they are recommended to verify the crack response.

The data acquisition system (DAS), used to collect crack response, was either a Somat 2000/2100 field computer system or a Somat eDAQ (*S*) (Somat Corp. 1999, 2001). For transient crack response, the sampling rate of the system was 1,000 samples/s. System resolution of the DAS was governed by either the resolution of the analog to digital (A/D) conversion or sensor resolution; however, in these cases the two were similar: between 0.65 and 0.083 μm per A/D division (unit). Long-term crack measurement was accomplished by measuring crack displacement once every hour. The time series of these "hourly" readings provides the long-term crack displacement time history. Development of vibration monitors to simultaneously measure long-term and transient crack response is underway at several manufacturers.

Sensors like those in Figs. 1 and 2 measure changes in the width of cracks shown in the inset. Results can be translated to total crack width by adding the initial width in Table 2 to all readings. Although crack extension potentially could be employed as a measure of crack response, it was not employed in this study. Henceforth in this paper, change in crack width will be referred to as crack displacement or more generally crack response.

Variation of Structures and Cracks Studied

Photographs of the seven structures are given in Fig. 3 and their plan views are illustrated in Fig. 4. They were located in Pennsylvania, New Mexico, Indiana, Illinois, Wisconsin, and Minnesota. Structure type varies widely and includes a double-wide trailer (*T*), an adobe brick ranch house (*A*), a bungalow with a concrete block basement (*B*), a highly distressed wood-framed house (*D*), a stone-faced, concrete block (CMU) house (*C*), a Victorian wood framed house (*V*), and a stucco-covered, tile block chapel (*S*). All structures were one story, except *V* and *S*, which were three, and all but *A* were founded on a basement.

Even though all of the cracks that were monitored were cosmetic in nature, their locations varied widely and involved a wide variety of material types. These cracks were chosen as the largest and most visible in the structure. As shown at the bottom of Table

Fig. 3. Seven structures monitored for crack response to long term and transient effects clockwise from top left: *T*, *A*, *D*, *V*, *S*, *C*, and *B*

2, the width of these cracks varied from 500 to 1,200 μm. Their plan locations are denoted as "crack sensor" in Fig. 4. Monitored cracks occurred in a variety of materials, and were located both inside and outside. They were located on interior drywall (*T* and *C*), interior plaster and lath (*D* and *V*), exterior concrete block (*B*), exterior stucco over adobe (*A*) and interior and exterior tile block (*S*).

The vibration environment varied widely for the structures in the study as shown in Table 1. Five (*T*, *A*, *B*, *D*, and *C*) were subjected to ground motions generated by either surface coal mine or aggregate quarry blasts. Maximum peak ground motions (in a direction parallel to the walls containing the cracks) ranged from 3.3 to 8.1 mm/s (0.13–0.32 ips), and generated responses that lasted between 1 and 7 s. These ground motions were such that they generated structural response velocities of 4.3–6.9 mm/s. Locations of transducers on the structure are illustrated in Fig. 5. Thus the values of structural amplification (the ratio of $S2$ from Table 1 divided by G) were as high as 1.5 and as low as 0.8. While the ratio of $S2/S1$ is important for wall strains, often amplification is described in terms of $S2/G$ and G and $S1$ are assumed to be equal. Dynamic crack response from occupant activity was recorded in *T*, *D*, *C*, and *V*.

Long-term (weather-induced) response of cracks was monitored at all seven of the structures for varying lengths of time. Structures *T*, *B*, and *D* were observed for 1 week or less, while *A*, *V*, *C*, and *S* were monitored for 1–3 months. Several of the longer study periods included a change in seasons (*V* and *S*), as well as extreme weather events (a rain storm in New Mexico, *A*).

The core of the responses in this paper, those from structures *T*, *A*, *B*, and *D*, were gathered during a study initiated by the Office of Surface Mining (OSM) (Aimone-Martin et al. 2002). These four structures were instrumented with velocity transducers (to measure dynamic structural response) in addition to crack sensors. Responses of the other three structures, *V*, *C*, and *S*, were

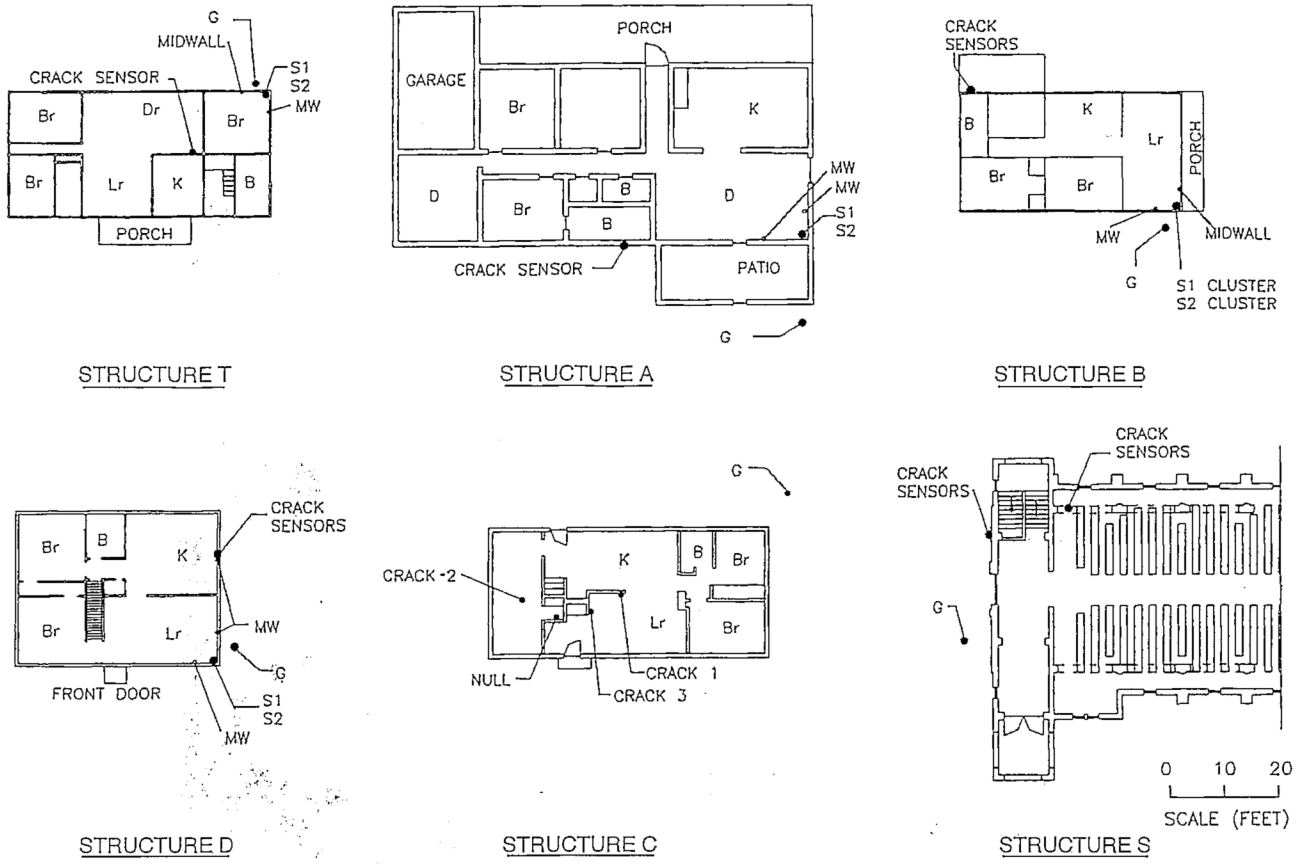

Fig. 4. Plan view of six structures monitored for crack response to long term and transient effects, clockwise from top left: structures *T*, *A*, *B*, *D*, *C*, and *S*

Table 1. Summary of Maximum Structural and Crack Response to Blasting

	Response						Ground motion			Blast	
	Maximum peak velocity parallel to cracked wall				Maximum crack response (μm)						
Structure, state wall cover (thickness, mm)	*G* (mm/s)	*S1* (mm/s)	*S2* (mm/s)	*S2*/*S1*	Dynamic	Weather	Peak frequency (Hz)	Peak particle velocity (mm/s)	Length of significant excitation (s)	Distance from crack (m)	Charge/ delay (kg)
Trailer, (*T*), Pennsylvania Drywall (102)	8.1	8.4	6.9	0.8	0.9	24	16.5	8.1	1.2	457	278
Ranch, (*A*), New Mexico Adobe (305)	3.3	2.8	4.3	1.5	4.2	25	6.2	3.6	7.1	1,506	4,359
Bungalow, (*B*), Indiana Concrete block (229)	4.6	3.3	5.2	1.6	0.3	12	28.4	5.8	5.8	438	205
Wood frame house, (*D*), Indiana Plaster/lath (152)	7.1	4.6	6.4	1.4	13.6	52	15	7.6	3.2	640	478
Block/stone house, (*C*), Wisconsin Drywall (152)	3.3	—	—	—	4.0	37	11	4.6	3.0	610	NA[a]
Victorian frame house, (*V*), Illinois Plaster/Lath (102)	—	—	—	—	40	100	—	—	—	—	—
Chapel, (*S*), Minnesota Stucco/tile (381)	—	—	—	—	—	107	—	—	—	—	—

[a]Not available.

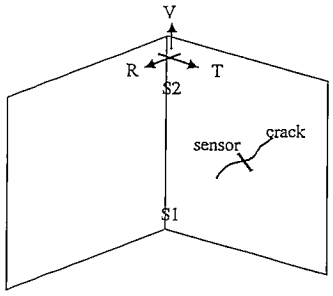

Fig. 5. Sketch of transducer placement in upper corner ($S2$) and orientation of transverse T, transducer in direction parallel to plane of the wall containing crack. Same scheme followed at lower corner ($S1$).

gathered during development of Autonomous Crack Measurement technology sponsored by the Infrastructure Technology Institute at Northwestern Univ. (Dowding and Siebert 2001; Louis 2000; Siebert 2000; and McKenna 2002). The project web page, http://www.iti.northwestern.edu/acm, Dowding (2005) allows access to archived sites, and background information. Only one of the latter three, C, was subjected to ground motions, as the focus of the work was the development of the crack monitoring technology.

Ground Motions and Structural Response

Excitation motions were measured with standard seismographs with particle velocity transducers, which respond linearly between 2 and 200 Hz, in two horizontal and one vertical direction (R, T, and V, respectively). These triaxial geophone blocks were typically located within 1–3 m of the structure, as shown in Fig. 4, and buried approximately 100–150 mm in the ground. The longitudinal direction R was oriented parallel to the long axis of the structure and the transverse direction was oriented parallel to the shortest dimension. An air overpressure (air-blast) transducer, which responded linearly down to 2 Hz, was installed on a 1 m high dowel for the OSM structures and affixed to the side of structures C and S (V was not instrumented with an air-blast transducer).

Response motions for the four OSM structures were measured at an interior corner of the house nearest the buried geophone block measuring excitation motions (shown in Fig. 4). As shown in Fig. 5, three transducers (R, T, and V) were located at the top ($S2$) and bottom ($S1$) of the corner. Seismograph $S1$, serviced three single-axis velocity transducers (R, T, and V) installed at the bottom corner of the structure and a second interior seismograph $S2$ serviced three single axis velocity transducers installed at the top corner of the structure. The indoor seismographs ($S1$ and $S2$) were linked to the outdoor seismograph (G) and all three were triggered simultaneously at a ground excitation threshold of 0.51 mm/sec (0.02 in./s) at the ground geophones. Each set of time histories was at least 7 s long, which was long enough to capture the entire event.

As shown in Fig. 5, motions "in the plane" of the wall containing cracks were those of transducers at the wall corner with sensitive axes parallel to the wall but mounted on the perpendicular wall. Velocity transducers were attached to walls within 20 or at most 50 mm of the corner. At the wall corner it was assumed that there would not be significant differences between motions measured with a transducer with its sensitive axis: (1) parallel to and on the wall or (2) parallel to but on the perpendicular wall. Transducers were mounted at the corners to ensure that the measured motions were predominantly those of the whole body or superstructure. This procedure of corner measurement follows that recommended by Siskind (2000).

Measured Response and Example

Fig. 6 compares crack displacement with velocity time histories of excitation ground motions and structure response to ground motion from a coal mining blast at the distressed, wood-framed Structure D. The 22 August blast consisted of 478 kg of Ammonium Nitrate-Fuel Oil (ANFO) per delay or instant, was initiated 640 m from the structure, and produced a peak crack displacement of 13.6 μm (535 μin.), with peak ground motion of 7.1 mm/s (0.28 in./s) parallel to the wall containing the crack (transverse T, in this case by study convention). Velocity time histories for the bottom, and top corners in the direction parallel to the wall containing the crack (as shown in Fig. 5) are labeled $S1(T)$ and $S2(T)$ in Fig. 6. Velocity measurements at the bottom ($S1$) and top ($S2$) corners were integrated to determine displacement time histories. The time history of the difference between the displacement values ($S1-S2$) was then plotted to show relative displacement, which is proportional to shear strain in the wall. These time histories show that wall response and excitation

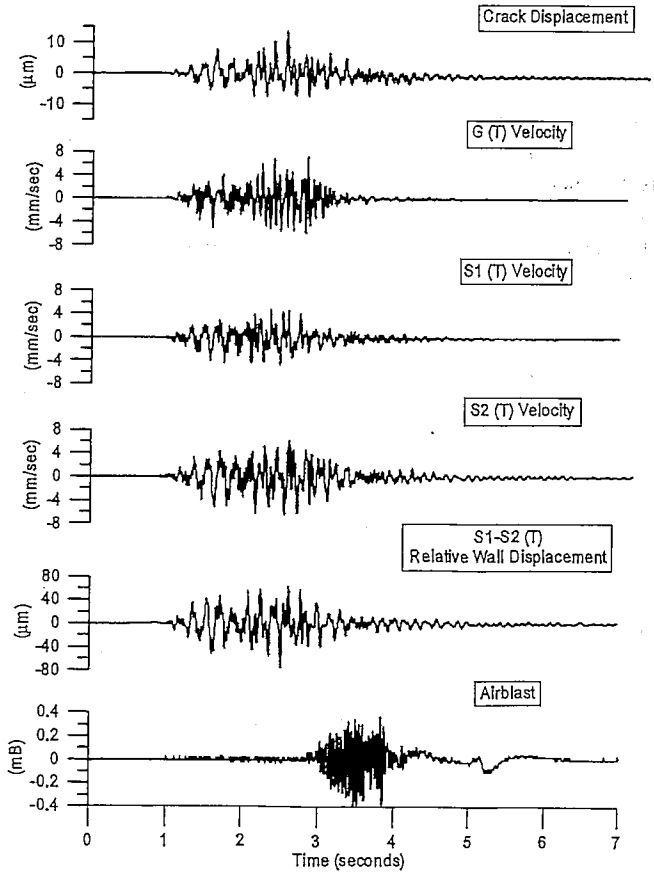

Fig. 6. Time histories of crack displacement in structure D on August 22, 2001 at 17:30 compared to velocity time histories in the transverse direction of ground (G), lower corner ($S1$), upper corner ($S2$), relative displacement of wall in transverse direction calculated by subtracting upper and lower displacement ($S1-S2$), and air-blast overpressure

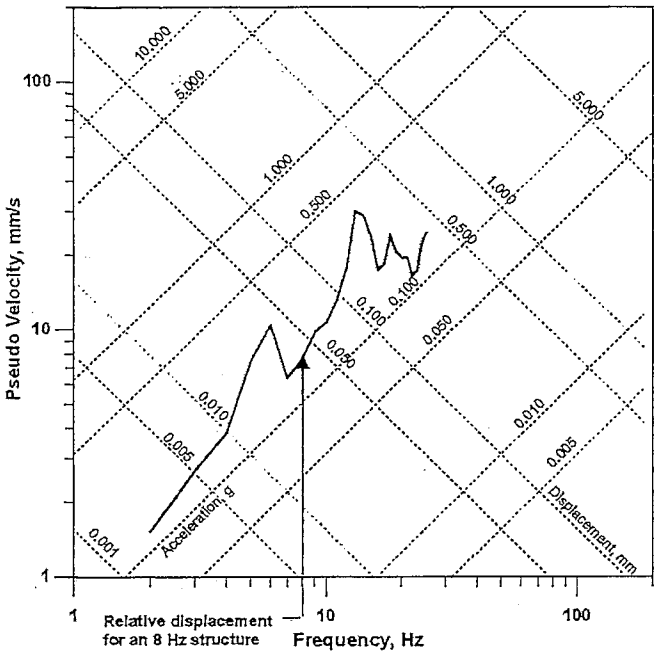

Fig. 7. Single degree of freedom response spectra of transverse motions produced by blast on August 22, 2001 at 17:30 showing dominant excitation frequency of 12–14 Hz and calculated relative displacement response of structure D with natural frequency of 8 Hz

motions are nonperiodic because of the multiple millisecond delayed detonations involved in any single "blast." Measured crack displacements are a fraction of the calculated relative structural displacements. Air-blast response is also included in this figure for comparison. While it played no role in this case, it can have a measurable effect on structures such as trailers. While space restrictions prevent inclusion of all 11 time histories, they have been archived and summarized in McKenna (2002).

The pseudovelocity response spectrum of transverse ground motions from the August 22, 2001 blast in Fig. 7 shows the dominant excitation frequency to be 12–14 Hz. The peak of the spectrum, 12–14 Hz, also shows that the dominant excitation frequency is greater than the 8 Hz natural frequency of the structure. The pseudovelocity spectrum gives the structural response in terms of relative displacement (plotted on the axis inclined toward the upper left) of a family of structures with common assumed damping of 5% but differing natural frequencies. The pseudovelocity plotted on the vertical, y axis is calculated from the relative displacement by assuming velocity is the relative displacement times two π times the structure's natural frequency. Hence the velocity axis is labeled "pseudovelocity." More information on this standard means of describing excitation frequency content and structural response can be found in any textbook on earthquake engineering and soil dynamics (e.g., Kramer 1996). The natural frequency of Structure D was ~8 Hz (McKenna 2002). Thus the calculated zero to peak displacement of the structure relative to the ground was 0.15 mm or 150 μm (5,900 μin.) measured on the axis inclined to the left at the intersection of the vertical 8 Hz line with the response spectrum. These are the relative displacements that are compared to measured crack displacement in a later section of this paper.

Crack Response to Long-Term Environmental Effects

Crack ("width") displacement response for the wood-framed house, D, is compared to the variation of weather indicators (temperature and humidity) in Fig. 8 to illustrate interrelationships for the house during its 3 days of observation. Complete sets of these observations, for all structures, are contained in McKenna (2002). Long-term crack displacement was measured hourly during the monitoring period, while temperature and humidity were measured every 10 min for OSM structures (T,A,B,D) and hourly for the others. From these once per hour values, two averages were calculated for comparison: (1) daily or 24 h moving average and (2) overall average during the period of observation.

Daily (24 h) average values of crack displacement (and temperature and humidity) were calculated as the average of the hourly measurements from 12 h before and 12 h after each hourly measurement. For example, at 12:00 p.m. on May 22, 2001, a 24 h average crack displacement was calculated from the 24 measurements recorded between 12:00 a.m. on August 23, 2001 to 12:00 on August 24, 2001. For the first and last 12 rolling averages computed, the first and last measurement recorded was counted more than once in the respective averages, in order to have 24 measurements included in every average.

Fig. 8 illustrates the manner in which the 1 h measurements, 24 h averages, and overall averages were used to determine crack response to weather effects. Longer periods of observation such as that in Fig. 9 will capture unusual storms as well as other effects such as foundation movements in response to seasonal changes in the water table. Weather effects have three distinct contributors: (1) frontal movements that change overall temperature and humidity for periods of several days to several weeks; (2) daily responses to changes in average temperature and solar radiation; and (3) extremes of unusual weather or other environmental effects. For purposes of this study the frontal effect is defined as the deviation of the peak 24 h moving average value from the overall computed average, the maximum of which is 28 μm (1,101 μin.) in this example. The daily effect is defined as the difference between the peak measurement and the 24 h average during any given day, which is 37 μm (1,455 μin.) in this example. The extreme (maximum) weather effect is defined as the difference between the peak measurement and the overall computed average, which is 52 μm (2,024 μin.).

Comparison of crack response to the changes in temperature and humidity in Fig. 8 shows that this crack responds to daily changes as well as the frontal effects. As humidity rises and temperature falls on both the daily and the longer term frontal bases, the crack displacement increases.

Comparison of Long-Term, Environmental, and Vibratory Crack Displacement

These specific observations at the distressed house, D, shown in Fig. 8, illustrate that weather effects are large compared to blast-induced effects. In order to highlight the relatively small responses associated with the blasts, the four resulting peak displacements are encircled in the figure. The maximum, dynamic crack displacement response of 13.6 μm or 537 μin. is approximately 1/4 of the 52 μm maximum weather effect response for just this 2 day period. This crack response is associated with a peak particle velocity (PPV) of 7.1 mm/s (0.28 in./s) in the transverse direction, which is parallel to the plane of the wall

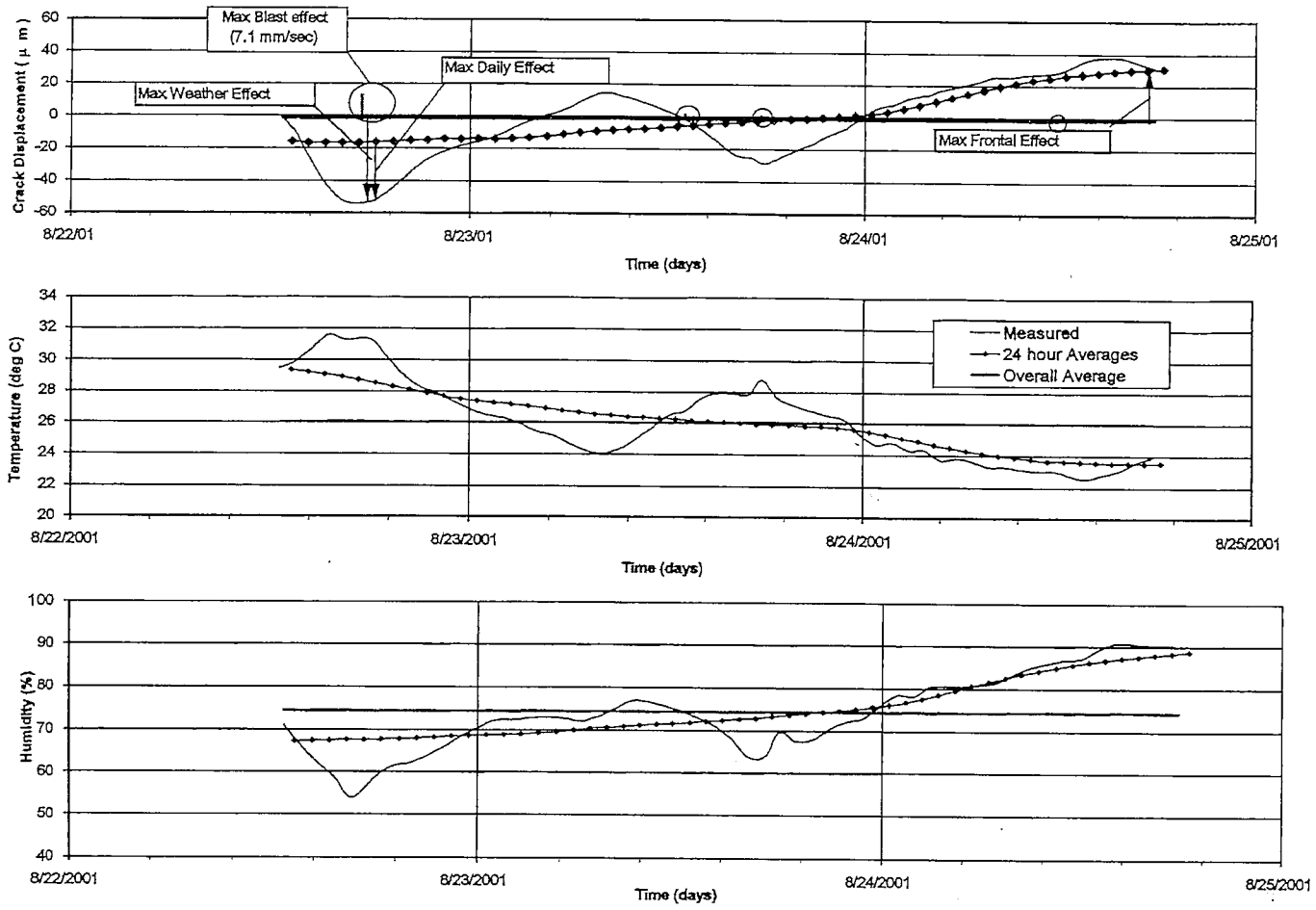

Fig. 8. Long term crack displacements compared to weather effects to illustrate method of distinguishing 24 h (daily), ~weekly (frontal), and maximum weather effects. Comparable zero to peak transient, blast, effects shown by bars

containing the crack. The maximum PPV for this event is 7.6 mm/s along the longitudinal axis. The three other encircled (and much smaller) vibratory crack responses resulted from blasts that produced PPVs of (1.2, 1.2, and 1.5 mm/s or 0.06, 0.06, and 0.05 in./s). The magnitude of each dynamic response corresponds to the absolute, maximum zero-to-peak displacement of the crack during the significant portion of vibratory motion. This zero to peak measure corresponds to the zero to peak particle velocity measure employed in past cracking research.

Longer periods of observation than the 2 days for this example will include larger weather effects. Fig. 9 shows long-term weather and blast-induced responses from a structure monitored for more than 6 months during the winter (Dowding 1996). Winter heating induced changes in crack width exceeded 40 μm. Blast-induced responses during the longer study in Fig. 9 were produced by surface, coal mine blasting vibrations that reached as high as 19.1 mm/s (0.8 ips). The relatively small dynamic response compared to the environmental effects in this comparison despite the high peak particle velocity further emphasizes the large difference in magnitude between weather response and blast-induced response of cracks.

Environmental and vibratory responses of cracks in all seven structures are compared in Table 2 and in Fig. 10. In addition to weather and vibratory crack responses, responses to occupant activities in structures *T*, *D*, *C*, and *V* are also included. The period of observation varied widely. As mentioned before, three of the four OSM structures were monitored for periods of 1 week or less. Structure *A* was observed for nearly 1 month. Observation of the others extended over 1, 3, and 4 months for structures *C*, *V*, and *S*, respectively. The length of monitoring each structure (in days) is presented at the bottom of Table 2.

For all five of the structures excited by blast-induced vibrations (*T*–*C*), maximum weather effects are at least ten times

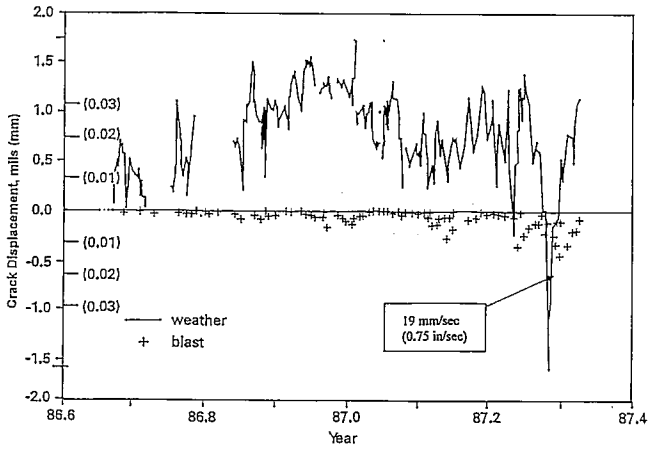

Fig. 9. Long term comparison of weather and blast-induced crack displacements during 9 months of observation from previous study (Dowding 1996)

Table 2. Comparison of Micrometer Crack Displacement Response to Environmental and Vibration Effects

Event	(*T*) Trailer interior drywall	(*A*) Ranch exterior adobe	(*B*) Bungalow exterior concrete block	(*D*) Distressed frame interior plaster/lath	(*C*) Block/stone interior drywall[a]	(*V*) Victorian frame interior plaster/lath[b]	(*S*) Chapel stucco exterior
	Displacement (μm)						
Maximum frontal effect	11	9	3	28	35	100	155
Maximum daily effect	16	25	9	37	15	20	100
Maximum weather effect	24	25	12	52	55	—	217
Max blast event (ppv in mm/sec)	0.9(8.1)	4.2(3.6)	0.3(5.8)	13.6(7.6)	5(4.6)	—	—
Blast event at 2.5 mm/sec	0.3	2	0.2	5	3	—	—
Slamming door (m)[c]	2.5(1.8)	—	—	1.6(4.3)	3.5(2.1)	10(1.5)	—
Jumping (m)	1.5(3.0)	—	—	1.9(4.9)	—	—	—
Hammering (m)	0.2(3.4)	—	—	2.2(0.3)	—	—	—
Shutting window (m)	—	—	—	4.1(0.9)	—	—	—
Walking on stairs	—	—	—	—	—	40	—
Foundation response (permanent)	—	16	—	—	—	—	—
Seasonal heating	—	—	—	—	—	300	—
Width of crack (μm)	700	800	500	1,200	500	500	1,000
Days of observation (ΔT in °C)	5 (7)	35 (29)	4 (17)	3 (9)	37 (25)	92 (23)	126 (35)

[a]Crack number 1 (Louis 2000).

[b]Crack number 2 located under stairwell (Seibert 2000).

[c]Distance to crack in meters

greater than the vibratory effects produced by ground motions that are widely noticeable, 2.5 mm/s (0.1 in./s). As described earlier, the maximum weather effect is defined as the maximum difference in the peak actual measurements from the overall computed averages of crack displacement during the study period. The vibratory response is the maximum, zero to peak crack displacement during the vibratory response. Both long-term, weather, and transient, vibratory, responses are measured by the same sensor, and thus are directly comparable.

As shown in Table 2, crack response to occupant activity can be as large as that produced by vibratory excitation that is distinctly perceptible (2.5 mm/s). Activities presented are a common

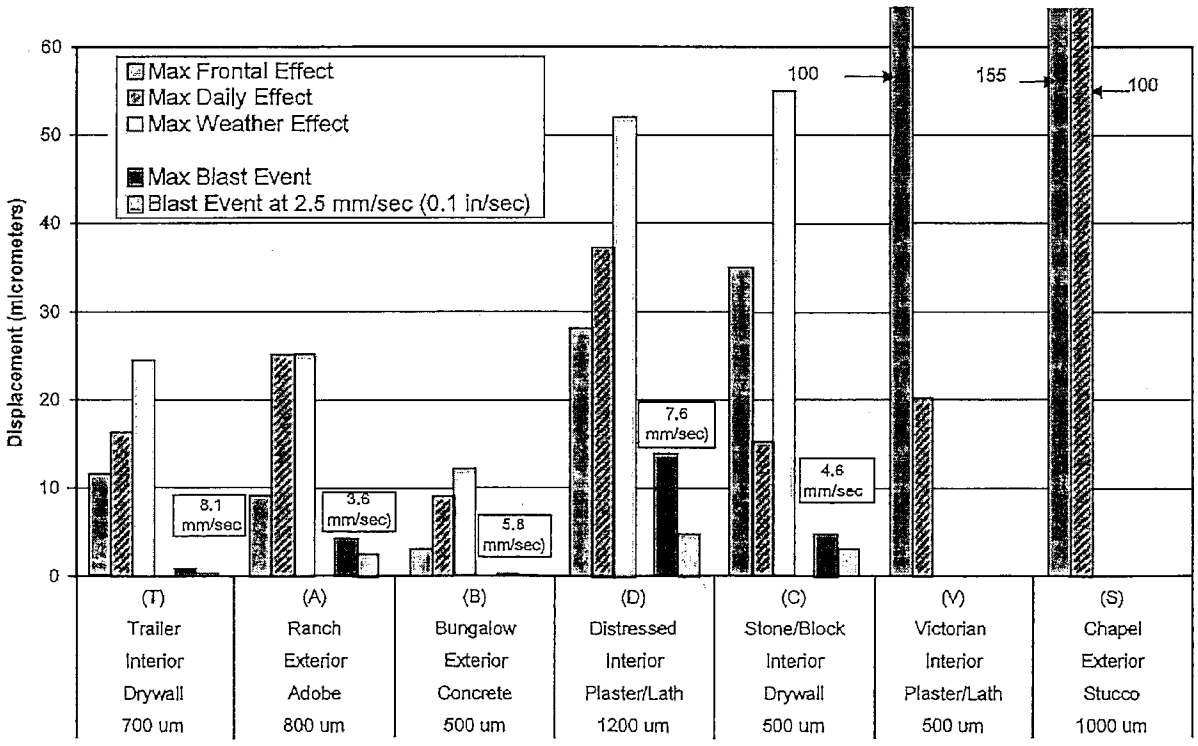

Fig. 10. Structure by structure comparison of measured crack displacements from long term weather effects (left three bars for each set) and vibratory, blast events (right two bars). Peak particle velocity in box is that of maximum blast event. Text below each set of bars describes each structure/house type, crack location, wall material, and total crack width

subset of the tests conducted at the five structures. Distances (m) from the crack to the location of the activity are shown along with the crack responses produced. Those activities closest to the crack produced the greatest response. The greatest response, 40 μm (1,575 μin.), was produced in Structure *V* by walking up a stairway (that may contain a construction defect), past the crack on the stairway wall.

Responses to two seasonal events, a rainstorm in New Mexico (Structure *A*) and seasonal heating in Illinois (Structure *V*), produced large and relatively permanent crack responses. These types of events typically are expected to be observed only for observation periods of 6 months or longer. The large magnitude and permanence of the crack responses point to the conclusion that seasonally extreme events produce even larger crack displacement than other events reported for most of the structures in this study. A 12 mm rainfall at the adobe home, *A*, which did not have a basement, produced a 16 μm (630 μin.) change that remained for the duration of the monitoring period (McKenna 2002). This permanent deformation is eight times greater than the 2 μm response of the crack to 2.5 mm/s, or noticeable, ground motions shown in Table 2. House heating during one winter heating season produced a 300 μm (12,000 μin.) crack displacement in Structure *V*, which is larger than the diameter of a human hair and 22 times the crack displacement produced by the largest particle velocity of 7.6 mm/s (0.28 in./s) at Structure *D*.

Comparison of Vibratory Crack Displacement with Structural Response from Velocity Measurements

It is instructive to compare measured crack response with the more traditional measures of cracking potential, to determine the similarity of the approaches. Traditionally ground motion is measured immediately adjacent to the structure. In limited cases where access to the structure is possible, structural velocity response is measured to deduce gross strain (Siskind 2000). In this case velocity responses are manipulated to calculate relative displacements (or strain) in the plane of the wall, which are then compared to critical levels. Computed relative displacements can be obtained with a number of methods such as the integration of velocity time histories, the single degree of freedom response spectrum method, and estimation based on sinusoidal approximation. Since crack displacements are measured in the plane of the wall containing the crack, comparisons are made with structural and wall responses measured in a direction parallel to the plane of the wall containing the crack (direction *T* for the example in Fig. 5).

Maximum measured crack displacements (*Y* axis) for each monitored blast response at structures (*T*, *A*, *B*, *D*, and *C*) are compared in Fig. 11 to the various estimates of peak structure or wall displacement (*X* axis). Also included is a comparison with the peak parallel ground motions, since ground motions are the regulatory index of the cracking potential. Within each of the six graphs, data for each house is labeled with the house letter, *A* and an =xx. The =xx is the correlation coefficient between the measured crack response and the estimate of wall/structure response. Correlation coefficients can "appear" to disagree with visual linearity for horizontal and vertical lines. While lines can be drawn through such data, there is low correlation.

The most direct measure of relative displacement involves subtracting perfectly time correlated (±0.001 s) pairs of integrated velocity time histories [upper corner, *S*2, minus lower corner, *S*1, or *S*2−*S*1, and *S*2 minus ground, *G*, or (*S*2−*G*)] to create a relative displacement time history. From the resulting time history, the peak relative displacement is determined for comparison with the measured crack displacement. Figs. 11(a and b) show the comparisons of peak measured crack displacements with the relative displacements calculated from pairs (*S*2−*S*1) and (*S*2−*G*), respectively. If structure response is not available, but ground motions are, a third, less precise index is sometimes calculated from the integrated ground particle velocity. The peak, integrated value is the maximum ground displacement. Fig. 11(c) shows a

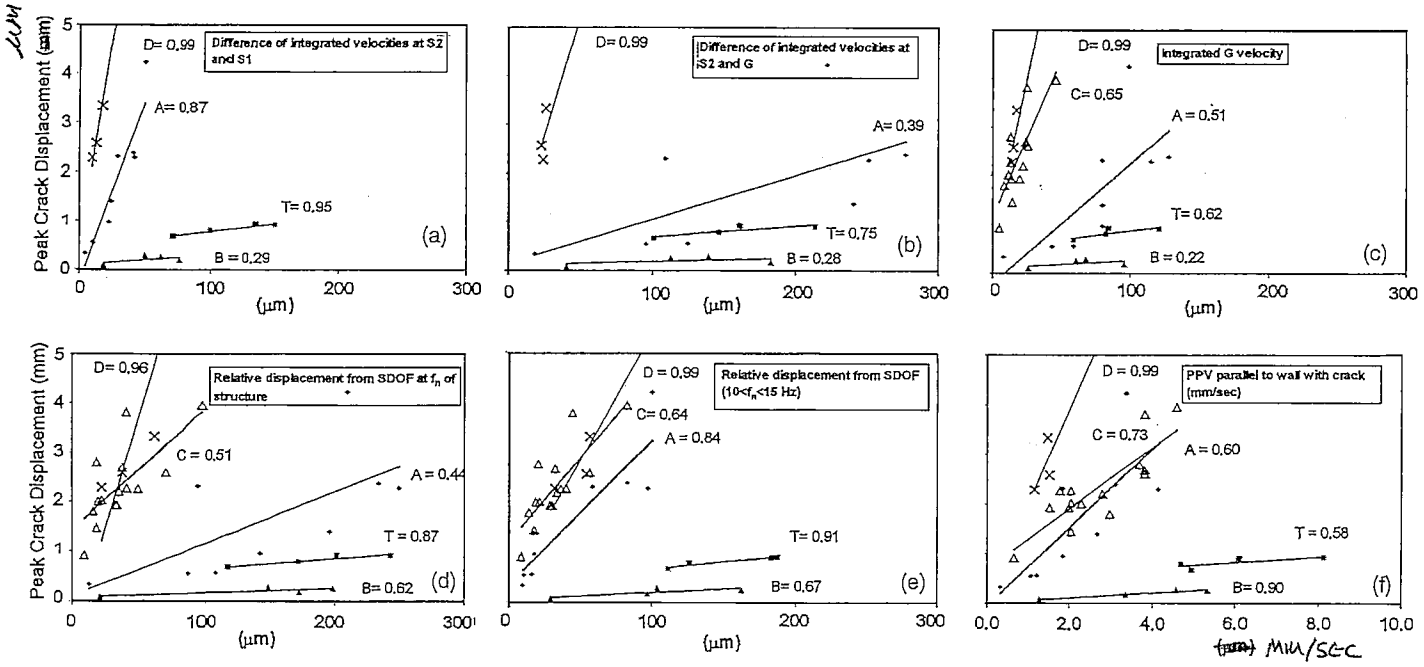

Fig. 11. Measured crack displacements (*Y* axis) compared to various means of estimating displacement (*X* axis) [plots (a)–(e)] as well as comparison with peak particle velocity parallel to wall [plot (f)]. Capital letters refer to house and =xx refers to correlation coefficient

comparison between peak crack displacements and the peak ground displacement.

Relative displacements can be estimated by calculating single degree of freedom (SDOF) relative displacement responses from the ground velocity time histories as described in Dowding (1996). A standard damping ratio of 5% was used for all calculations in this paper. Estimated relative displacements are found from either: (1) the SDOF relative displacement response at the dominant frequency of the superstructure [Fig. 11(d)] or (2) the average of SDOF responses between 10 and 15 Hz [Fig. 11(e)]. Average values of natural frequencies for typical residential structure walls range between 10 and 15 Hz. Since cracks are located on walls that can respond to both superstructure and wall motions, depending on the design of the walls and the ground motions, both approaches were taken to estimate a relative displacement associated with the ground motion.

Comparison of measured crack displacements with peak particle velocity (PPV of ground motions) is presented as Fig. 11(f).

Discussion

Differences in relations between measured crack and structural response are small compared to the large impact of weather related response, as demonstrated above. Changes in crack width produced by ground motions with maximum PPVs between 3 and 8 mm/s were less than 5 μm, except in one instance; whereas, the maximum weather responses during 1 week (or shorter) periods of observation were 10–50 μm. The crack in Structure *D* that showed the largest motion response (13.6 μm) also showed the largest weather response (52 μm).

Of all of the estimates of response, measured crack displacement correlated best with the difference in integrated velocity time histories of the upper and lower corners, ($S2-S1$). This correlation is shown in Fig. 11(a). This higher correlation was expected, as ($S2-S1$) is the relative displacement of the wall, which is proportional to the gross, in-plane, shear strain in the wall. In a sense, this calculated difference also could be considered as a direct measurement of the wall strain when measured at the upper and lower elevations of a single story wall of constant cross section. In Fig. 11 correlation coefficients can "appear" to disagree with visual linearity for horizontal and vertical lines. While lines can be drawn through them, there is low correlation. Structure *B*'s responses are an example. The crack in *B* was very narrow, located in the CMU foundation, and had the lowest dynamic response of all the cracks.

The second best correlation with measured crack displacement is obtained from the pseudovelocity response spectrum (PVRS), with the average of responses between 10 and 15 Hz. The PVRS is a derivative of calculated relative displacement that accounts for the structural response frequency, as well as the full excitation time history (Siskind et al. 1980; Dowding 1996). These correlations, shown in Fig. 11(e), are almost identical to those between the two direct measures of relative wall displacement or strain ($S2-S1$ and $S2-G$). This frequency range lies between the natural frequency of superstructures and walls. Correlations are lower with PVRS displacements for the estimated dominant frequency associated with each superstructure.

Dual-purpose sensors described herein could be placed across a crack to simultaneously measure long-term and vibratory changes in crack width to augment the traditional approach of measuring particle velocity to control construction vibrations. This augmentation might be helpful in some instances where blasting or construction vibrations occur for sustained periods of time, as many complainants who believe that construction vibrations disturb their homes or buildings tend to focus their discussion on cosmetic cracks like that in Fig. 1. Because they interpret the response of buildings through their senses they tend to believe that if the vibrations can be felt and associated with noise heard, there could be a negative effect on the structure.

Traditionally complaints are addressed by measuring peak particle velocity outside the structure of concern with a blasting or vibration seismograph. In limited circumstances structural motions are also measured. These measured peak ground motions are then compared with standards developed by federal or state government agencies. Motions that people truly believe are harmful usually turn out to be below these government standards, which are viewed with skepticism. Additional measurement of crack response would allow comparison between the effects of the "silent crackers"—temperature, humidity, long term distortion, material changes, etc.—to the phenomena that is felt and heard—blasting and construction effects such as pile driving.

Conclusions

This paper summarizes measurements of response of cosmetic cracks to long term effects as well as blast-induced ground motions in seven structures. Crack sensors employed in this study allowed simultaneous measurement of both long-term (environmental or weather induced) and vibration (blast or occupant induced) changes in crack width in a wide variety of wall materials. Cosmetic cracks monitored in this study occurred in: (1) exterior stucco over adobe bricks and tile blocks, as well as concrete masonry units and (2) interior plaster and lath, as well as dry wall. Structures were framed with wood, concrete masonry units, and tile block, and included a trailer, an adobe ranch, wood Victorian, a concrete block, and stone faced house, as well as a tile block chapel.

Long-term cosmetic crack response to weather induced changes was measured in all seven of the structures over periods of 3–126 days. Three of the seven structures were monitored for 5 days or less and most likely did not capture the effects of significant changes in weather. The long-term response was subdivided into effects caused by: (1) daily changes, (2) passage of weather fronts occurring over a period of days, and (3) extremes of unusual weather or other environmental effects.

Measured vibration-induced movements of cosmetic cracks in the five structures subjected to blast-induced peak particle velocities between 3 and 8 mm/s were compared with a wide range of estimates of the wall distortion. These vibratory responses were also compared to the long term responses and those produced by ground motions at low but noticeable peak particle velocities of 2.5 mm/s.

The synthesis of these measurements and calculations leads to the following conclusions. More work and measurements are needed to generalize these conclusions.

1. Long-term response of the cosmetic cracks monitored in these case studies is at least 4–5 times larger than the vibratory response at maximum measured peak particle velocities and more than 7–10 times larger than vibratory response at low but noticeable levels.
2. Extreme events such as rain storms in desert climates, long and intense changes in humidity, and seasonal heating can cause permanent and/or extreme crack responses that are

much larger than those induced by typical daily and weekly weather changes.

3. Vibratory crack response induced by household activities can approach or exceed the vibratory response to low but noticeable peak particle velocities.
4. Crack displacements induced by typical changes in weather and distinctly perceptible vibrations are far smaller than the width of the cosmetic cracks.
5. Measured crack displacements correlate best with the difference in structural displacement of the top and bottom corners of the single story wall containing the crack. These estimated displacements come from integrated and time correlated velocity time histories of structure motion in the plane of the wall containing the crack.
6. Measured crack displacements also correlated well with estimates made from ground motions that take into account the time history of the excitation and response characteristics of the structure using the single degree of freedom method.
7. Measurements of crack response with adjacent LVDT and eddy current displacement sensors (across the same crack) showed a constant proportional dynamic response between the two. Thus either sensor type is appropriate for this type of study provided low drift sensors are employed.

Acknowledgments

Support of a large number of individuals and organizations was necessary for this project; their cooperation is deeply appreciated and gratefully acknowledged. The Infrastructure Technology Institute (ITI) at Northwestern University, directed by David Schulz, has supported development of Autonomous Crack Monitoring technology through a grant from the Department of Transportation. Two members of the ITI instrumentation staff, Daniel Marron and David Kosnik, played key roles in the development of the ACM hardware and software. Results not presented herein are chronicled in three Northwestern University MS theses by Damien Siebert, Michael Louis, and Laureen McKenna. Intensive instrumentation of the four "atypical" structures summarized herein was made possible through the cooperation of the Department of the Interior's Office of Surface Mining (OSM) program to measure response of "atypical" structures. Ken Eltschlager, Dennis Clark, and Mike Rosenthal, as well as a number of representatives from supporting state agencies, provided extensive field support for the OSM program. Finally, without the fieldwork, instrumentation and sharing of data by Professor Cathy Aimone-Martin and Mary Alena Martell of the New Mexico Institute of Mining and Technology results presented herein would not exist.

References

Aimone-Martin, C., Martell, M.-A., McKenna, L. M., Siskind, D. E., and Dowding, C. H. (2002). *Comparative sudy of structure response to coal mine blasting*. Prepared for Office of Surface Mining Reclamation and Enforcement Appalachian Regional Coordinating Center, Pittsburgh, Pa. ⟨http://hpa.osmre.gov/arblast/downloads/StructureResponse.pdf⟩

Dowding, C. H. (1996). *Construction vibrations*, Chap. 13, Prentice-Hall, Upper Saddle River, N.J.

Dowding, C. H. and Seibert, D. (2001). "Control of Construction Vibrations with an Autonomous Crack Comparometer," *Explosives and Blasting Technique*, R. Holmberg, Ed., A. A. Balkema, pp. 103-110

Dowding, C. H. (2005). "Continually updated project web site for the Autonomous Crack Monitoring Project," Infrastructure Technology Institute and Department of Civil and Environmental Engineering, Northwestern Univ., Evanston, Ill.

Kramer, S. L. (1996). *Geotechnical earthquake engineering*, Prentice–Hall, Upper Saddle River, N. J.

Louis, M. (2000). "Autonomous crack comparometer phase II." MS thesis, Northwestern Univ., Evanston, Ill.

McKenna, L. (2002). "Comparison of crack response in diverse structures to dynamic events and weather phenomena." MS thesis, Northwestern Univ., Evanston, Ill. ⟨www.iti.northwestern.edu/acm⟩

Siebert, D. (2000). "Autonomous crack comparometer." MS thesis, Northwestern Univ., Evanston, Ill.

Siskind, D. E., Stagg, M. S., Kopp, J. W., and Dowding C. H., (1980). *Structure response and damage produced by ground vibration from blasting*, United States Bureau of Mines, Report of Investigations, *8507*, 74.

Siskind, D. E. (2000). *Vibrations from blasting*, International Society of Explosives Engineers, Cleveland.

Somat Corporation (1999). *Somat TCS for Windows, version 2.0*, Champaign, Ill.

Somat Corporation (2001). *Somat TCE eDAQ, version 3.5.1*, Champaign, Ill.